Contents lists available at ScienceDirect

Biomedicine & Pharmacotherapy

journal homepage: www.elsevier.com/locate/biopha

S-allylmercapto-N-acetylcysteine ameliorates pulmonary fibrosis in mice via Nrf2 pathway activation and NF-κB, TGF-β1/Smad2/3 pathway suppression

Qinxiu Zhang [a,b], Wenhui Ye [a,b], Ying Liu [a,b], Decao Niu [a,b], Xin Zhao [a,b], Genjv Li [a,b], Ying Qu [a,b], Zhongxi Zhao [a,b,c,d,*]

[a] Department of Pharmaceutics, Key Laboratory of Chemical Biology of Ministry of Education, School of Pharmaceutical Sciences, Cheelloo College of Medicine, Shandong University, 44 West Wenhua Road, Jinan, Shandong 250012, PR China
[b] Key University Laboratory of Pharmaceutics & Drug Delivery Systems of Shandong Province, School of Pharmaceutical Sciences, Cheeloo College of Medicine, Shandong University, 44 West Wenhua Road, Jinan, Shandong 250012, PR China
[c] Pediatric Pharmaceutical Engineering Laboratory of Shandong Province, Shandong Dyne Marine Biopharmaceutical Company Limited, Rongcheng, Shandong 264300, PR China
[d] Chemical Immunopharmaceutical Engineering Laboratory of Shandong Province, Shandong Xili Pharmaceutical Company Limited, Heze, Shandong 274300, PR China

ARTICLE INFO

ABSTRACT

Pulmonary fibrosis (PF) is a chronic lung disease characterised by alveolar inflammatory injury, alveolar septal thickening, and eventually fibrosis. Patients with severe Coronavirus Disease 2019 (COVID-19) may have left a certain degree of pulmonary fibrosis. PF is commonly caused by oxidative imbalance and inflammatory damage. S-allylmercapto-N-acetylcysteine (ASSNAC) exhibits anti-oxidative and anti-inflammatory effects in other diseases. However, the pharmacodynamics of ASSNAC remain unclear for PF. This investigation aimed to evaluate the efficacy and mechanism of ASSNAC against PF. The PF model was established by TGF-β1 stimulating HFL-1 cells *in vitro*. ASSNAC exhibited the potential to inhibit fibroblast transformation into myofibroblasts. Also, in the PF mice model with bleomycin (BLM), the sodium salt of ASSNAC (ASSNAC-Na) inhalation was treated. ASSNAC remarkably improved mice's lung tissue structure and collagen deposition. The important indicator proteins of PF, collagen I, collagen III, and α-SMA significantly decreased in the ASSNAC treated groups. Besides, ASSNAC attenuated oxidative stress by reversing glutathione (GSH), superoxide dismutase (SOD) levels and interfering with Nrf2/NOX4 signaling pathways. ASSNAC showed an anti-inflammatory effect by reducing the number of inflammatory cells and inflammatory cytokines, such as TNF-α and IL-6, and blocking the NF-κB signaling pathway. ASSNAC inhibited fibroblast differentiation by blocking the TGF-β1/Smad2/3 signaling pathway. This study implicates that ASSNAC alleviates pulmonary fibrosis through fighting against oxidative stress, reducing inflammation and inhibiting fibroblast differentiation.

1. Introduction

Pulmonary fibrosis (PF) is a chronic progressive lung disease that is characterized by extracellular matrix (ECM) deposition and myofibroblast activation. In this condition, the lung tissue becomes irreversible scarred over time, which leads to lung function decline [1–3]. PF is

---

mostly occurring people with age between 50 and 70 years old [4]. It is similar to cancers with high mortality rate and the median survival time is only 2–5 years [5]. PF is one of the lung injury characteristics in the patients with severe COVID-19 and the autopsy results of the first case of COVID-19 showed severe PF [6]. Therefore, it is important to investigate safe and effective treatment strategies for PF.

The research shows that oxidation imbalance, inflammatory injury, and excessive accumulation of ECM result in PF [7,8]. Bleomycin (BLM) induces oxidative stress by increasing reactive oxygen species (ROS) and subsequent DNA damage [9–11] and subsequently causes inflammatory response and triggers the activation of transforming growth factor β1 (TGF-β1), the major cytokine causing tissue fibrosis [12]. GSH and SOD are the crucial component of antioxidant defence systems. Hence, increasing the contents of GSH and SOD are helpful to fight against oxidative stress. Nicotinamide adenine dinucleotide phosphate oxidase 4 (NOX4), the main enzyme for regulating oxidative stress, is overexpressed in pulmonary diseases. Oxidative stress induced by NOX4 can regulate the fibroblasts' differentiation by TGF-β [13]. Nrf2 activation is a key defense mechanism against oxidative stress. Under normal conditions, Nrf2 is sequestered by repressor Kelch−like ECH−associated protein 1 (Keap1) in the cytoplasm and promotes its ubiquitination [14]. Under stress conditions, oxidants and electrophiles can covalently modify the reactive cysteine residues in Keap1, resulting in the conformation changes of Keap1 that inactivate the Keap1 −Cul3 E3 ligase [15,16]. Nrf2 is released from Keap1 and translocates to the nucleus to induce the transcription of downstream genes [17,18]. The up-regulation of NOX4 and down-regulation of Nrf2 exhibite continuous redox imbalance, which shows that NOX4 and Nrf2 play a key role in PF [19,20].

Nuclear factor kappa-B (NF-κB) regulates the transcription of many genes related to inflammation, cell apoptosis, and proliferation [21]. Inhibitor kappa B alpha (IκB-α) is a cytoplasmic inhibitor of NF-κB, inhibiting the production of pro-inflammatory cytokines such as interleukin-6 (IL-6) and tumor necrosis factor-α (TNF-α) and causing anti-inflammatory responses [22,23]. Therefore, inhibiting the NF-κB signaling pathway could be a potential treatment target for PF. TGF-β1 is closely related to inflammation, immune response, and matrix synthesis [24,25]. TGF-β1 can activate the Smad2/3 signaling pathway, and the phosphorylation of Smad2 and Smad3 further promotes the expression of TGF-β1 and pro-fibrotic genes [26]. Also, the TGF-β1/Smad2/3 pathway is the key to linking oxidative stress and inflammation signaling pathways. Therefore, inhibiting TGF-β1/Smad2/3 signaling pathway is beneficial to fight against PF [27]. A large number of studies have reported that oxidative stress caused inhibiting Nrf2 pathway, inflammation caused activating NF-κB pathway and fibrosis caused activating TGF-β1/Smad2/3 pathway are three key pathways in PF initiation and deterioration [28–30]. Therefore, anti-oxidation and anti-inflammatory have become the new therapeutic strategy to fight against PF [31].

Aerosol treatment can precisely deliver drugs to the lungs, which is an appropriate strategy for pulmonary diseases. The lungs have a rich capillary network and a thin alveolar epidermal cell layer, which acts as unique advantages for improving bioavailability [32]. Compared with oral administration, pulmonary drug delivery can reduce adverse effects on the gastrointestinal tract and avoid the first-pass effect, thus enhancing the drug bioavailability.

Acetylcysteine (NAC), a commonly used thiol-containing antioxidant, plays an anti-fibrotic effect by providing GSH, eliminating ROS antagonistic oxidative damage and improving the antioxidant effect of the organism. The previous research has shown that NAC has an anti-fibrotic effect on rats [33]. However, the bioavailability of NAC is very low and more than 600 mg doses per day needed to be provided to combat GSH deficiency caused by oxidative stress [34,35]. It was reported that N-acetylcysteine amide (NACA) increased bioavailability by 6–7 folds and GSH replenishing capacity by 3–4 folds than NAC [36]. S-allylmercapto-N-acetylcysteine (ASSNAC), containing NAC or NACA

structure, could also provide GSH and resist oxidative stress [37]. Therefore we chose NAC as the positive control in this experiment.

ASSNAC is the derivative of allicin, which plays an important role in anti-oxidation, anti-inflammation, and against chronic obstructive pulmonary disease (COPD) [37–39]. S-allylmercaptocysteine (SAMC) is an analogous structure of ASSNAC and exhibits an anti-fibrotic effect [40]. However, the efficacy and mechanism of ASSNAC against PF in vitro *and in vivo* has not been reported yet. In this study, ASSNAC aerosol inhalation was developed to assess its therapeutic efficacy and mechanism for PF. Our research demonstrated that ASSNAC fought against PF by anti-oxidantive and anti-inflammatory mechanisms. All these studys provide the potential future application of ASSNAC for PF treatment.

2. Material and methods

2.1. Drugs and reagents

ASSNAC (purity ≥96%) was synthesis of our laboratory based on earlier reports [41,42]. To improve the solubility of ASSNAC, ASSNAC-Na salt was made before the experiments. NAC was obtained from Beyotime Biotechnology (Shanghai, China). BLM was acquired from Shanghai Yuanye biology Co., Ltd (Shanghai, China). Fetal bovine serum (FBS) was received from Biological Industries (Beit Haemek Ltd., Israel). F12K medium was bought from M&C Gene Technology Co., Ltd (Beijing, China). TGF-β1 was received from PeproTech Co., Ltd (PeproTech, USA). The enzyme-linked immunosorbent assays (ELISA) kits were obtained from Shanghai Multi Sciences Biotech Co., Ltd (Shanghai, China). BCA protein assay kit was bought from biosharp Co., Ltd (Guangzhou, China). Commercial assay kits for SOD and GSH were obtained from Nanjing Jiancheng Bioengineering Research Institute Co., Ltd (Nanjing, China). Antibodies against IκBα, NF-κB p65, and p-NF-κB p65, α-SMA, TGF-β1, Smad2/p-Smad2, Smad3/p-Smad3, and collagen I were received from Cell Signaling Technologies (Danvers, MA, USA). Anti-NOX4 was purchased from Proteintech Group Inc. (Chicago, IL, USA). Anti-GAPDH Anti-Nrf2 and anti-HO-1 were obtained from Abcam (Cambridge, UK). Anti-collagen III was acquired from Bioss Biotechnology Co., Ltd (Beijing, China). Sirius Red was obtained from Macklin Co., Ltd (Macklin, China). Wright-Giemsa reagent was purchased from Solarbio Biotechnology Co., Ltd (Solarbio Biotechnology, Beijing, China). All other chemicals used were of analytical grade.

2.2. Cell cultures and PF model in vitro

The Human fetal lung fibroblast 1 (HFL-1) cells were received from BeNa Culture Collection (HeBei, China; source: ATCC) and cultured in an F12K medium containing 10% FBS at 37 ℃ using an incubator with 5% CO$_2$/95% air.

Before experiments, HFL-1 cells were starved for 12 h to maintain a low basal level of α-smooth muscle actin (α-SMA) expression. Cells were then treated with ASSNAC-Na for another 48 h after 3 h treatment with TGF-β1 (5 ng/mL). The grouping settings were: Control group: cultured in a medium; Model group: first incubated with TGF-β1 for 3 h and then cultured for another 48 h in a medium; Treatment groups of ASSNAC: first stimulated with TGF-β1 (5 ng/mL) for 3 h and then cultured in different concentrations of ASSNAC (30 μM, 60 μM, 90 μM) for another 48 h; Positive control group: first stimulated with TGF-β1 (5 ng/mL) for 3 h and then cultured in NAC (200 μM) for another 48 h. Western blot analysis was then carried out to determine the related protein expressions of PF.

2.3. MTT assay

The viability of HFL-1 cells was investigated by MTT assay after treating different concentrations of ASSNAC for 24 or 48 h. Briefly, 20 μL MTT solutions (5 mg/mL) was added to each well and incubated for 4 h at 37 ℃. Subsequently, after removing the supernatant, the formed blue

for mazan crystals were dissolved using DMSO (150 µL per pore). Cell viability was tested by measuring the optical density (OD) at 490 nm using the microplate reader (Infinite® M200 PRO, TECAN, Switzerland).

2.4. Wound healing and collagen protein staining experiments

Wound healing experiments were carried out according to the previous study [43,44]. HFL-1 cells were cultured in a 6-well plate, and a scratch was made across the cell monolayer of the cultured well using a sterile 200 µL micro-pipette tip. Then, HFL-1 cells were treated with ASSNAC (90 µM) and TGF-β1 (5 ng/mL), and the cells were incubated in an F12K medium without FBS for 12 h at 37 ℃ in 5% CO₂. The scratch was observed and captured under an inverted optical microscope at 0, 6, and 12 h (Microscope: IX71, Olympus, Japan). The widths of the scratch were analyzed by Image J software and the percentages of the migration rates were compared respectively. The migration rate was calculated using the following Eq. (1).

$$Migration rate(\%) = 1 - \frac{scratched distance(6/12h)}{scratched distance(0h)} \times 100\% \quad (1)$$

Collagen protein staining was performed as described previously [45]. HFL-1 cells were seeded into 6-well plates at 10,000 cells/well in a 2 mL culture medium without FBS for 12 h at 37 ℃ in 5% CO₂. They were then treated with TGF-β1 (20 ng/mL) for 3 h, followed by ASSNAC (90 µM) treatment, and cultured for another 72 h in a medium. The cells were stained using Sirius Red, and the images were recorded under an inverted optical microscope. Image J software was used to assess the results, and the staining area was calculated.

2.5. Experimental animals

Adult male SPF C57BL mice (8–9 weeks, 20–23 g) were bought from Jinan Pengyue Experimental Animal Breeding Co., Ltd (Jinan, China). All mice were kept at 20–25 ℃ with a humidity of 45~60% RH with a 12 h light/dark cycle. The mice were given free access to water and food and received 7 days of adaptive feeding before experiments. All our experimental protocols were approved by the Animal Care and Use Committee of Shandong University (No. 2016020, Jinan, Shandong, China).

2.6. Grouping and modeling

30 mice of C57BL/6 were randomly divided into five different experimental groups: Control group (C); Model group (BLM, 5 mg/kg), Low dose ASSNAC (25 mg/kg, L), High dose ASSNAC (50 mg/kg, H), Positive control group (NAC, 100 mg/kg). Except for the control group that received intratracheal saline, other mice received BLM injection intratracheally (5 mg/kg) on 0 day. From 1–28 days, mice were inhaled with ASSNAC-Na or NAC daily. Control and model groups mice inhaled the same saline volume. The weight changes of mice were recorded every two days during the experimental period. After 28 days, the mice were used for the experiments.

2.7. Histopathological and immunohistochemistry experiments

For histological analysis, the left middle lungs were harvested, fixed by 4% paraformaldehyde for 24 h, dehydrated in ethyl alcohol, and cut into a slice of 5 µm thickness. The slice was stained with Hematoxylin and Eosin (H&E) and Masson's Trichrome to evaluate the pathological changes in the lungs. Image J software was used to analyze Masson's staining results.

The expressions of α-SMA, NOX4, TGF-β1, and p-Smad2 in lung tissues were studied by immunohistochemistry analysis. In brief, the sections were dewaxed, and rehydrated, and the antigen was retrieved with citrate buffer. To eliminate nonspecific binding, the samples were incubated with 1% serum in PBS at 37 ℃ for 30 min. Following

blocking, the sections were incubated with rabbit antibodies against anti-α-SMA, anti-TGF-β1, anti-NOX4, and p-Smad2 overnight at 4 ℃. The secondary antibody with HRP-labeled goat was incubated, and a DAB detection kit was used to visualise finally. The microscope was used to photograph these sections at 400 × (Eclipse, Nikon, Japan). Image J software was used to assess the results, and the average optical density (AOD) was calculated.

2.8. Analysis of relevant indicators of bronchoalveolar lavage fluid (BALF) and lung tissue

After treatment, in each group of mice, BALF was collected with 0.8 mL saline three times. All BALF was centrifuged at 1000 rpm for 10 min at 4 ℃. The supernatant of BALF was collected and stored at − 80 ℃ to analyze TGF-β1, IL-6 and TNF-α further. The cells were resuspended in 100 µL PBS solution. Total cells were counted using a hemocytometer. Under light microscopy, to distinguish macrophages and neutrophils, Wright-Giemsa stain was used to resuspend the PBS solution. The number of macrophages and neutrophils were calculated based on different cell morphologies under the microscope.

The tissue was homogenised by adding sterile physiological saline under an ice bath, and 10% tissue homogenate was obtained. The lung tissue homogenate was centrifuged at 3500 rpm for 10 min at 4 °C, and the obtained supernatant was used for analysis. The GSH and SOD levels were examined using the commercial kits.

2.9. Western blot analysis

The HFL-1 cells and mouse lung tissue proteins were extracted using radio immunoprecipitation assay (RIPA) buffer containing 1% phenyl-methyl sulfonyl fluoride (PMSF). The proteins were determined using a BCA protein assay kit. Equal quantities of proteins were separated by SDS-PAGE and then transferred onto polyvinylidene fluoride (PVDF) membranes (Millipore Corp., Billerica, MA, USA). The membranes were blocked with 5% defatted milk powder in tris buffer solution tween (TBST) at room temperature for 1.5 h and incubated with primary antibodies overnight at 4 ℃ with shaking subsequently. After being washed three times for 10 min with TBST, the membranes were incubated with HRP-labeled goat-anti-rabbit/ mouse IgG antibody for 1 h at room temperature. They were washed three times again with TBST for 10 min. The protein band intensity was measured with the Image LabTM software (Bio-Rad, Hercules, USA).

2.10. Statistical analysis

All experimental data were analyzed by origin 8.5 and GraphPad Prism 6.0 software. Numerical data are shown as the mean ± standard deviation (SD) for at least triplicate experiments. Tukey's test and ANOVA were used for statistical analysis, and $p < 0.05$ indicates statistical significance.

3. Results

3.1. Effect of ASSNAC on the proliferation of HFL-1cells and migration of TGF-β1-induced HFL-1cells

The cytotoxic effect of ASSNAC on HFL-1 cells was examined by the MTT assay. As shown in Fig. 1A and B, ASSNAC is not cytotoxic to HFL-1 cells in the range of 0–120 µM after culturing for 24 and 48 h. Hence, it did not affect HFL-1cells viability at 120 µM or less in the subsequent experiments. The activated fibroblasts migration occurs in the preliminary stage of injury repair and promotes PF development [46,47]. Thus, a wound-healing assay was used to evaluate the effects of ASSNAC on the migration of TGF-β1induced fibroblasts. HFL-1 cells were treated with TGF-β1 (5 ng/mL), followed by ASSNAC (90 µM), and cultured for 6, 12 h. As shown in Fig. 1C and D, ASSNAC inhibits the migration of
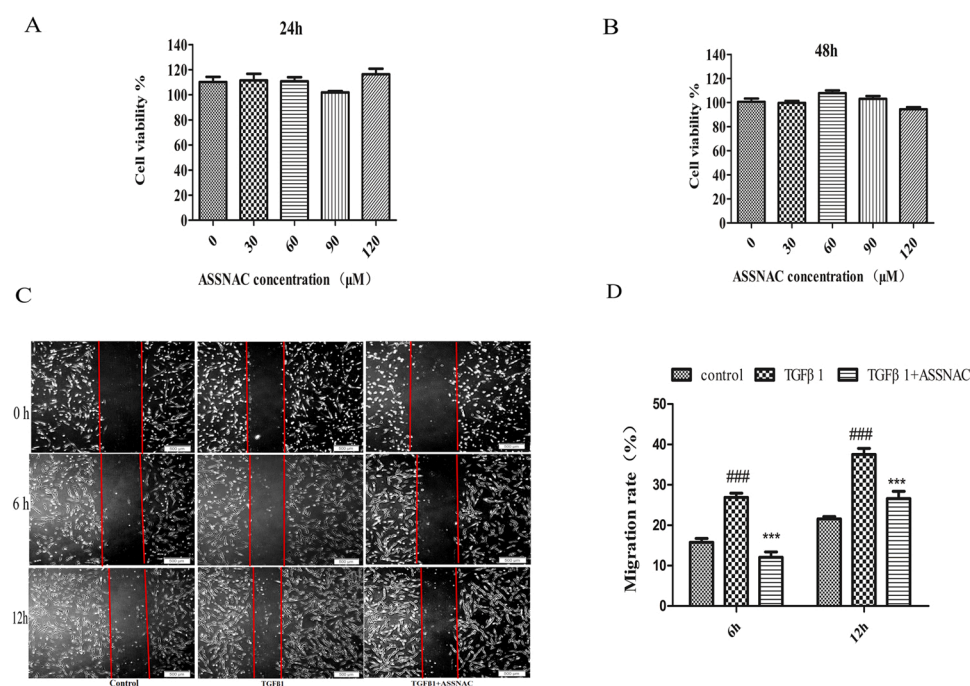
A

24h

B

48h

C

D

A

B

C

D

E

Fig. 2. Effect of ASSNAC on the expressions of collagen I and α-SMA and collagen deposition in HFL-1cells stimulated with TGF-β1 *in vitro*. Collagen I and α-SMA protein expressions were investigated by Western blot analysis with TGF-β1 induction and ASSNAC treatment in HFL-1cells (A-C). Sirius red staining of HFL-1 cells, Control group: without TGF-β1 and ASSNAC; TGF-β1 group: treat with TGF-β1; Treatment group: treat with TGF-β1 and ASSNAC (D). Scale: 200 μm (100 ×), 100 μm (200 ×). Semi-quantitative analysis of collagen staining area (E). Data are expressed as the mean ± SD (n = 3). ##p < 0.01, ###p < 0.001 vs the control group; *p < 0.05, **p < 0.01, ***p < 0.001 compared with the TGF-β1 group.

HFL-1 cells induced with TGF-β1.

3.2. ASSNAC inhibits the expression of α-SMA, collagen I, and collagen deposition in HFL-1 cells stimulated with TGF-β1 in vitro
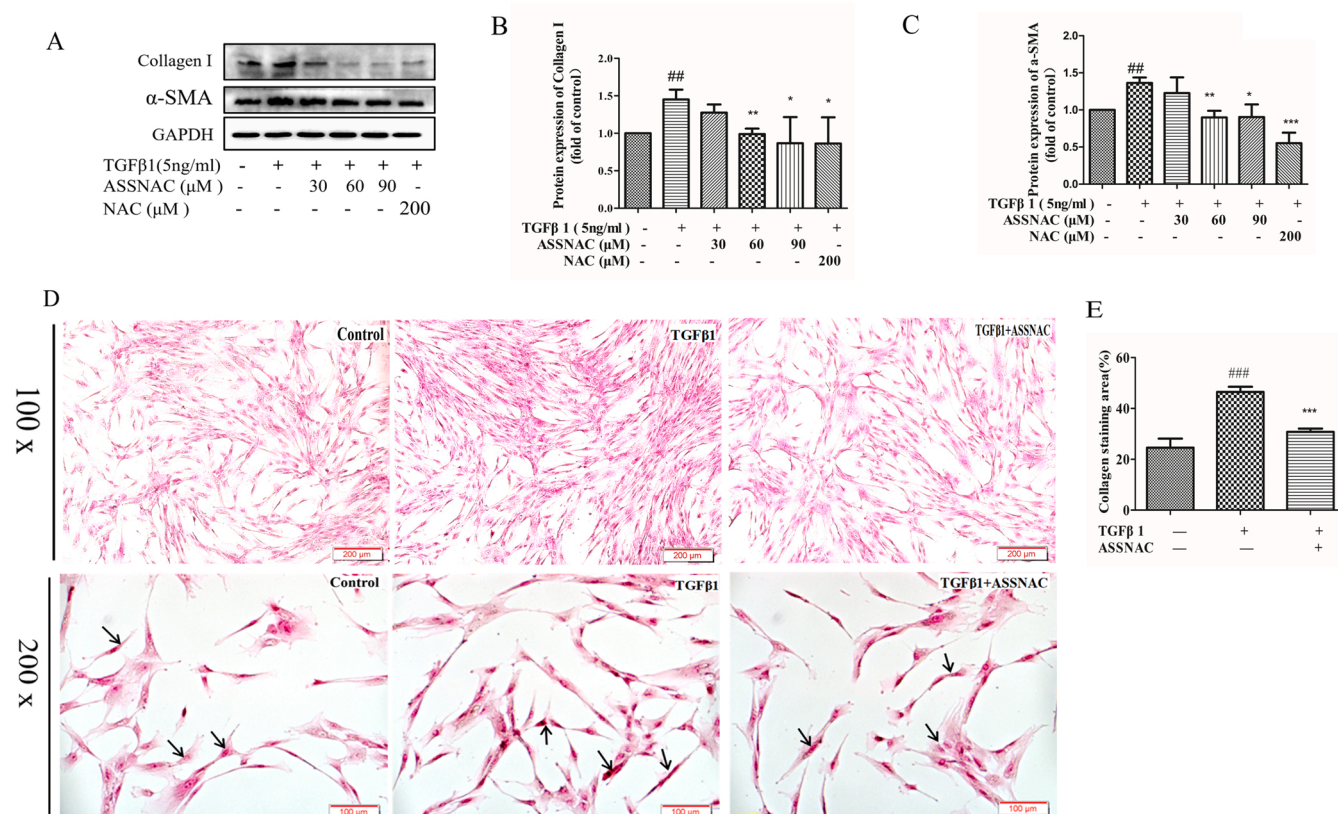
To further examine the inhibitory effect of ASSNAC, HFL-1 cells were induced by TGF-β1 and then treated with ASSNAC (30 μM, 60 μM, 90 μM) or NAC. NAC plays anti-fibrotic role as its antioxidant and anti-inflammatory effects [40]. Since ASSNAC has chemical structures similar to that of NAC, we used NAC as the positive control in this experiment. The protein expression of α-SMA, a typical activation marker, and collagen I were tested by Western blot analysis. The experimental results show that the protein expression levels of α-SMA and collagen I dramatically increase in HFL-1 cells stimulated with TGF-β1 compared with the control group. On the other hand, the expressions of α-SMA and collagen I decrease significantly after ASSNA and NAC treatments (Fig. 2A-C).

Collagen deposition is the main characteristic of PF. To explore the ASSNAC effect on collagen deposition, 20 ng/mL TGF-β1 was added to HFL-1 cells cultured in 6-well plates, followed by ASSNAC (90 μM) for 72 h. The collagen protein was then stained in the treated HFL-1 fibroblasts. Collagen protein staining in the control group was mainly concentrated around the cell nucleus and had the lighter staining. However, the model group with 20 ng/mL TGF-β1 increased the staining intensity, and the collagen deposition was widely distributed throughout the cytoplasm. The collagen protein staining intensity was

reduced in the ASSNAC (90 μM) co-treatment group than in the TGF-β1 group (Fig. 2D, E). These changes could be observed more clearly and was marked in the Fig. 2D (200 ×). Therefore, ASSNAC inhibits the collagen deposition in HFL-1 cells stimulated with TGF-β1.

3.3. ASSNAC ameliorates BLM-induced PF

As shown in Fig. 3A, B, hematoxylin-eosin and Masson's trichrome staining were used to estimate the alveolar architecture and lung fibrosis, respectively. Fig. 3A shows no damage in alveoli structures with clear alveolar sacs in the control group. In the BLM group, BLM administration in mice shows the destruction of normal alveoli structures, degeneration of interalveolar septa, thickening, and the infiltration of inflammatory cells in the alveolar spaces. However, the mice lung receiving ASSNAC and NAC improved significantly compared with the BLM group.

Masson's trichrome staining, an important indicator of collagen deposition and fibrosis, was carried out. As shown in Fig. 3B, no obvious ECM deposition and fibrosis could be seen in the control group; however, in the BLM group, a significant amount of ECM deposition occurs along with fibrosis. The treated groups with ASSNAC and NAC significantly reduced ECM and collagen strength compared with the BLM group. This outcome is also supported by the statistical results of the PF area (Fig. 3C). Hence, ASSNAC significantly decreased pulmonary inflammatory injury and collagen deposition by BLM, which is beneficial to ameliorating pulmonary function.
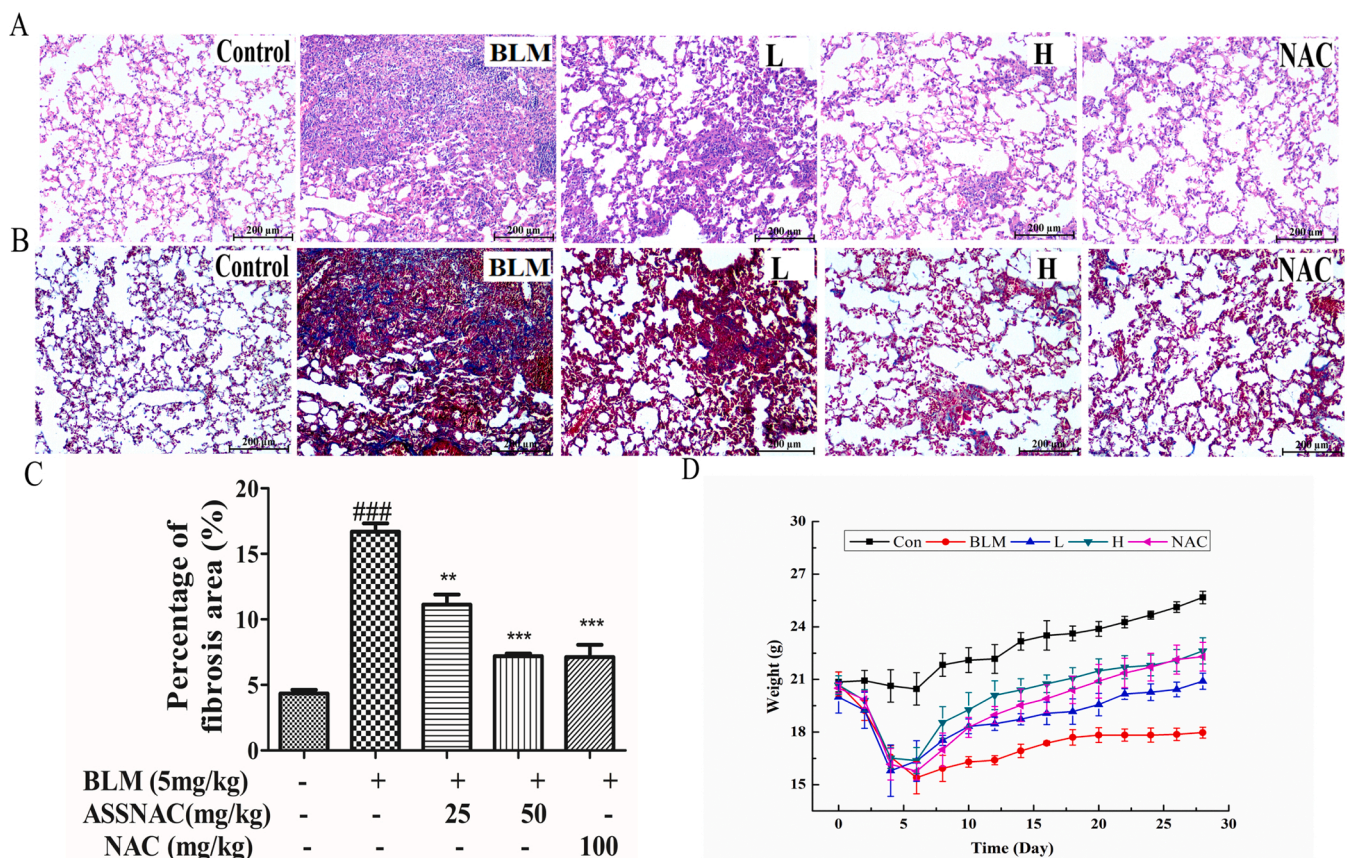
Fig. 3. ASSNAC ameliorated BLM-induced mice PF. The mice lung tissue specimens were stained with hematoxylin-eosin (H&E) (A) and Masson's trichrome (B) to estimate alveolar architecture and lung fibrosis. Scale: 200 μm. (C) Masson's trichrome staining to analyze fibrosis area. (D) The changes in mice weight during the study period. Group settings are: Control group: administered saline by inhalation; BLM group: the mice received intratracheal BLM injection of 5 mg/kg on day 0, and then administered saline by inhalation; Treatment groups: the mice received intratracheal BLM injection of 5 mg/kg on 0 day, and then administered saline containing ASSNAC 25 mg/kg (low dose, L), 50 mg/kg (high dose, H) and NAC (100 mg/kg) by inhalation for 28 days. Data are shown as the mean ± SD (n = 3). ###p < 0.001 vs the control group; **p < 0.01, ***p < 0.001 vs the model group.

The changes in mice's weight were recorded during the study to investigate the side effects of different treatments. As shown in Fig. 3D, in the control group receiving intratracheal saline and inhaled saline, the body weights slightly decreased within the first 7 days, and then the body weights smoothly increased until the end of this study. The groups with BLM-induced body weights constantly decreased for the first 7–10 days. In contrast, the body weights in the therapeutic groups that inhaled ASSNAC or NAC were higher than the model group after 7–10 days. Thus, ASSNAC alleviated mice PF by reducing lung inflammatory injury and collagen deposition.

3.4. ASSNAC decreases the related protein expressions of lung fibrosis

Collagen deposition in lung tissue is the most obvious pathological feature of PF patients. Collagen I and collagen III play a key role in developing PF. The protein expressions of collagen I and III in the BLM-induced PF mice were examined by Western blot analysis (Fig. 4A, B, D, E). The results reveal that collagen I and III protein expressions were increased in the model group than in the control group. However, collagen I and III contents were remarkably decreased in the ASSNAC or NAC treatment groups than in the model group in a dose-dependent manner.

The α-SMA protein is an important sign of the transformation of fibroblasts into myofibroblasts. The α-SMA expression was detected by Western blot and immunohistochemical analyses. An obvious increase in the expression of α-SMA is shown in the BLM-induced mice lung PF model group, and ASSNAC decreases the expression of α-SMA (Fig. 4A, C, F, G). Consequently, ASSNAC alleviates PF by inhibiting the expression of major PF proteins.

3.5. ASSNAC palliates PF by anti-oxidative effects in the lungs of BLM-induced mice

Oxidative imbalance is the main reason for PF. The GSH and SOD levels are the key indicators for evaluating anti-oxidant capacity. To investigate the anti-oxidative effect of ASSNAC during PF, the GSH and ROS contents were determined in mice lung tissue samples. As shown in Fig. 5A and B, compared with the control group, the GSH and SOD levels in the lungs of BLM-induced mice decreased. In comparison, ASSNAC and NAC both remarkably improved the GSH and SOD levels. This shows that ASSNAC plays an anti-oxidative role in PF treatment.

3.6. ASSNAC activates Nrf2/NOX4 signaling pathway in vivo and in vitro and exerts anti-oxidative effects

Clinical studies indicate that excessive NOX4 expression leads to PF, which could be relieved by inhibiting NOX4 [48]. Nrf2, a transcription factor, induced various cytoprotective enzymes expression, including HO-1. The Nrf2 signaling activation is important to maintain cellular homeostasis and inhibiting oxidative stress [49]. The expressions of Nrf2 and HO-1 were activated, which reduced oxidative stress. Hence, NOX4 down-regulation and Nrf2 up-regulation contribute immensely to recovering the body's oxidation-reduction balance and indirectly inhibiting PF formation. To investigate the molecular mechanism of ASSNAC in anti-oxidation, the marker proteins (Nrf2, HO-1, and NOX4) were analysed in vitro *and in vivo* by Western blotting and immunohistochemical analyses. The vitro experiment results displayed that protein expression levels of Nrf2 and HO-1 were remarkably decreased in the model group that HFL-1 cells stimulated with TGF-β1 than control
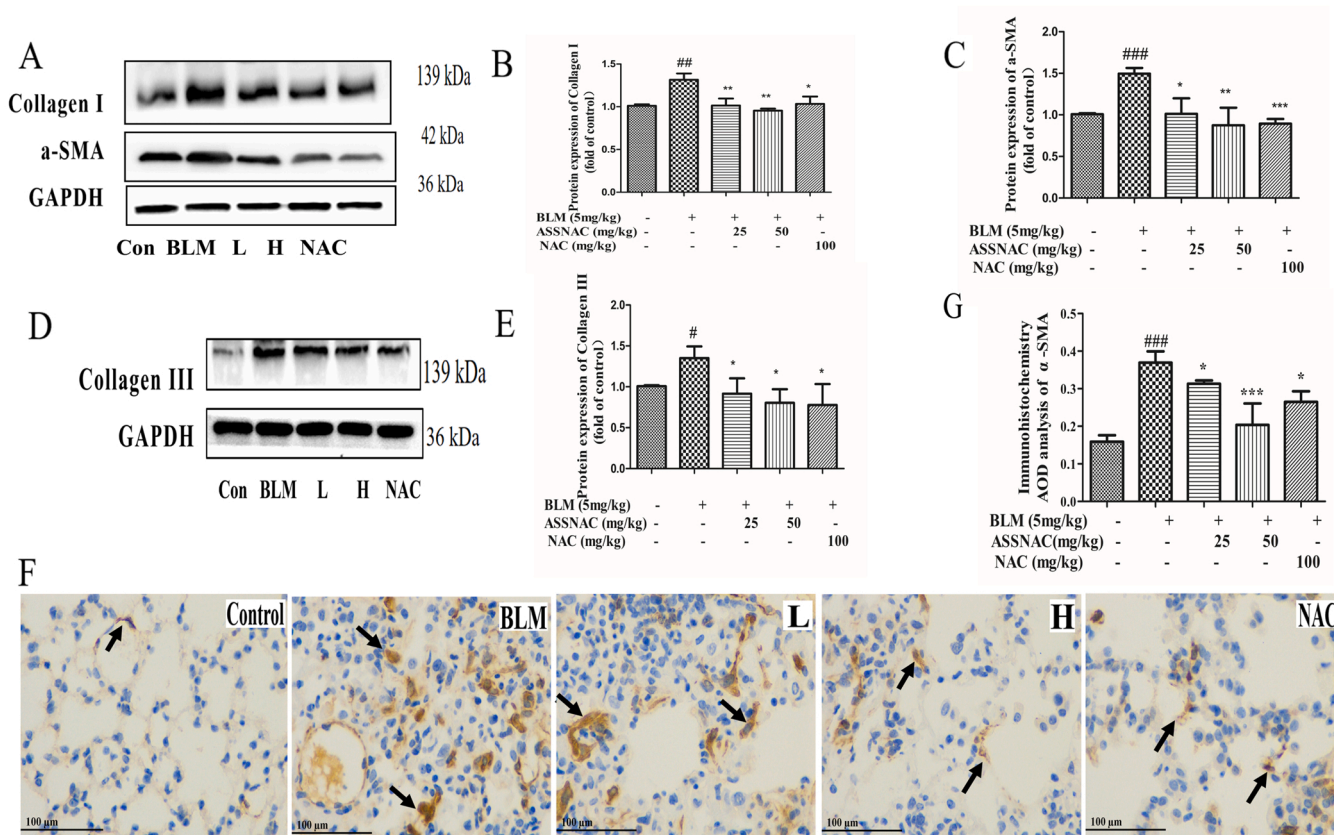
Fig. 4. Effect of ASSNAC on the related protein expressions of lung fibrosis *in vivo*. (A-E) α-SMA, collagen I, and collagen III proteins expressions were estimated by Western blot analysis in mice lungs with BLM induction and ASSNAC treatments. (F) α-SMA was stained brown by immunohistochemical analysis. Scale: 100 μm. (G) The immunohistochemistry AOD analysis of α-SMA. Data are shown as the mean ± SD (n = 3). #p < 0.05, ##p < 0.01, ###p < 0.001 compared with the control group; *p < 0.05, * *p < 0.01, * **p < 0.001 compared with the BLM group.

Fig. 5. Effect of ASSNAC on the GSH and SOD levels in fibrosis mice *in vivo*. (A) The GSH level in lung tissue. (B) The SOD level in lung tissue. Data are represented as the mean ± SEM (n = 3). #p < 0.05, compared with the control group; *p < 0.05, * *p < 0.01, * **p < 0.001 vs the model group.

group, while the group treatment with both ASSNAC and NAC reversed these changes (Fig. 6A-C). The level of NOX4 was increased in the TGF-β1 group than control group, while the group treatment with both ASSNAC and NAC remarkably decreased in a dose-dependent manner. (Fig.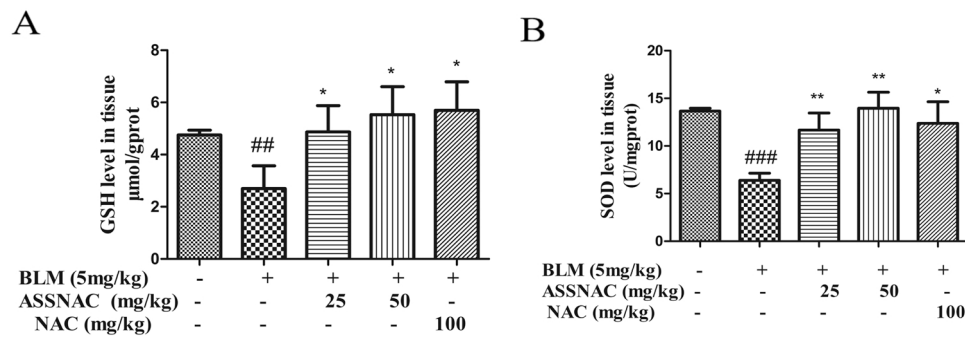 6D-E). *In vivo,* the results show that the expressions of Nrf2 and HO-1 decrease, while NOX4 significantly increases in the mouse lung tissue induced with BLM by Western blot analysis. However, ASSNAC reversed the expression of oxidative/anti-oxidative factors (Fig. 7A-E). Immunohistochemical analysis of NOX4 presents similar results (Fig. 7F, G). Hence, ASSNAC plays an anti-oxidative role by blocking NOX4 and activating the Nrf2 pathway. Studies demonstrate ASSNAC amelioration

of PF through the anti-oxidative signaling pathway.

3.7. ASSNAC ameliorates PF by reducing inflammation

To further investigate the anti-inflammatory activity of ASSNAC, the inflammatory cells in BALF were collected and counted by Wright-Giemsa staining. As shown in Fig. 8A, Neutrophils were stained lavender and macrophages were stained navy blue. In Fig. 8B, the number of total cells, neutrophils and macrophages were counted. In the BLM group increased dramatically than in the control group. However, the number of cells, including total cells, macrophages, and neutrophils,

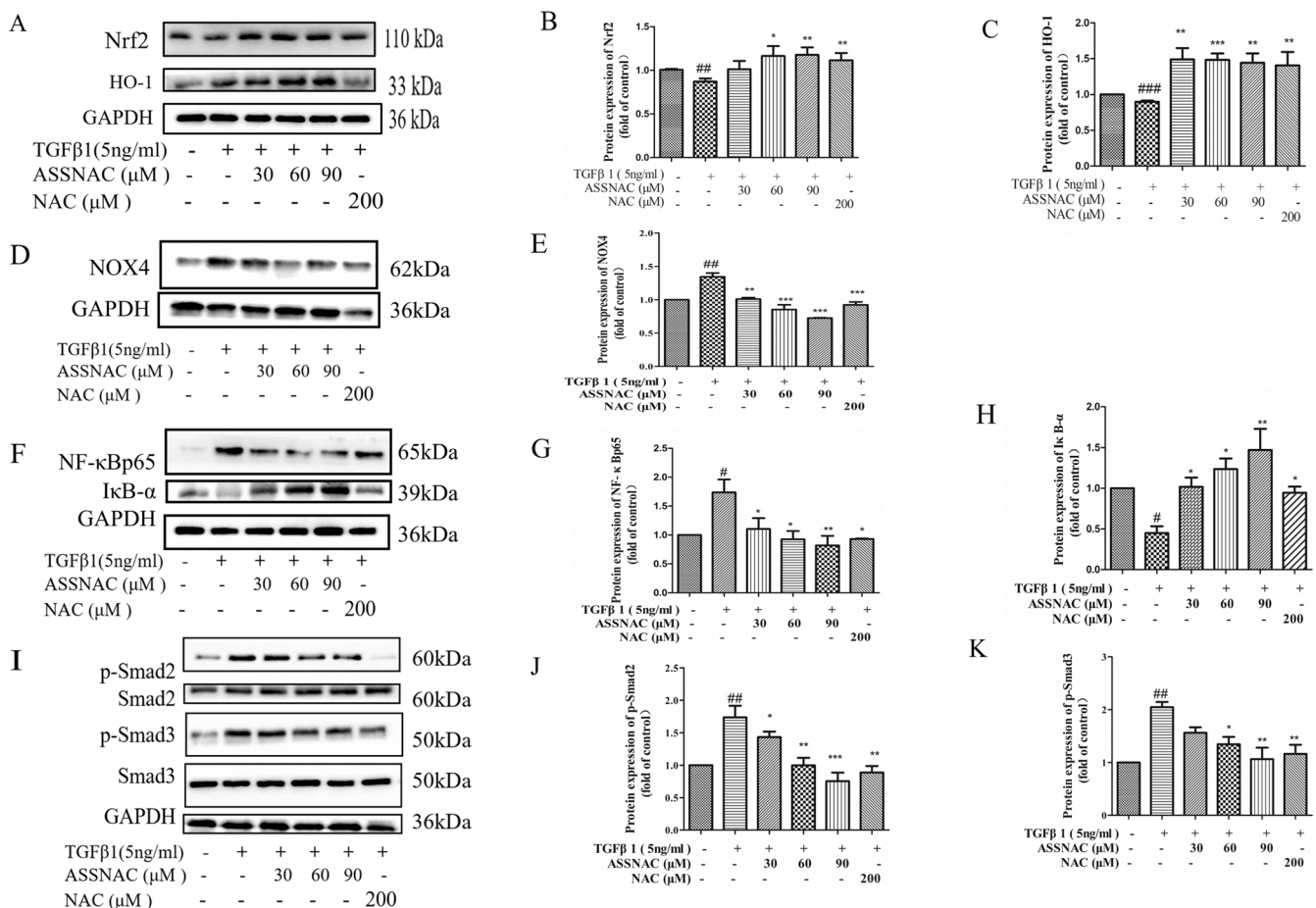**Fig. 6.** The effect of ASSNAC against fibrosis through Nrf2, NF-κB and TGF-β1/Smad2/3 signaling pathway *in vitro*. The expressions of proteins were estimated by Western blot analysis with TGF-β1-induced and ASSNAC treatment in HFL-1cells. Data are shown as the mean ± SD (n = 3). #p < 0.05, ##p < 0.01, ###p < 0.001 compared with the control group; *p < 0.05, * *p < 0.01, * **p < 0.001 vs the model group.
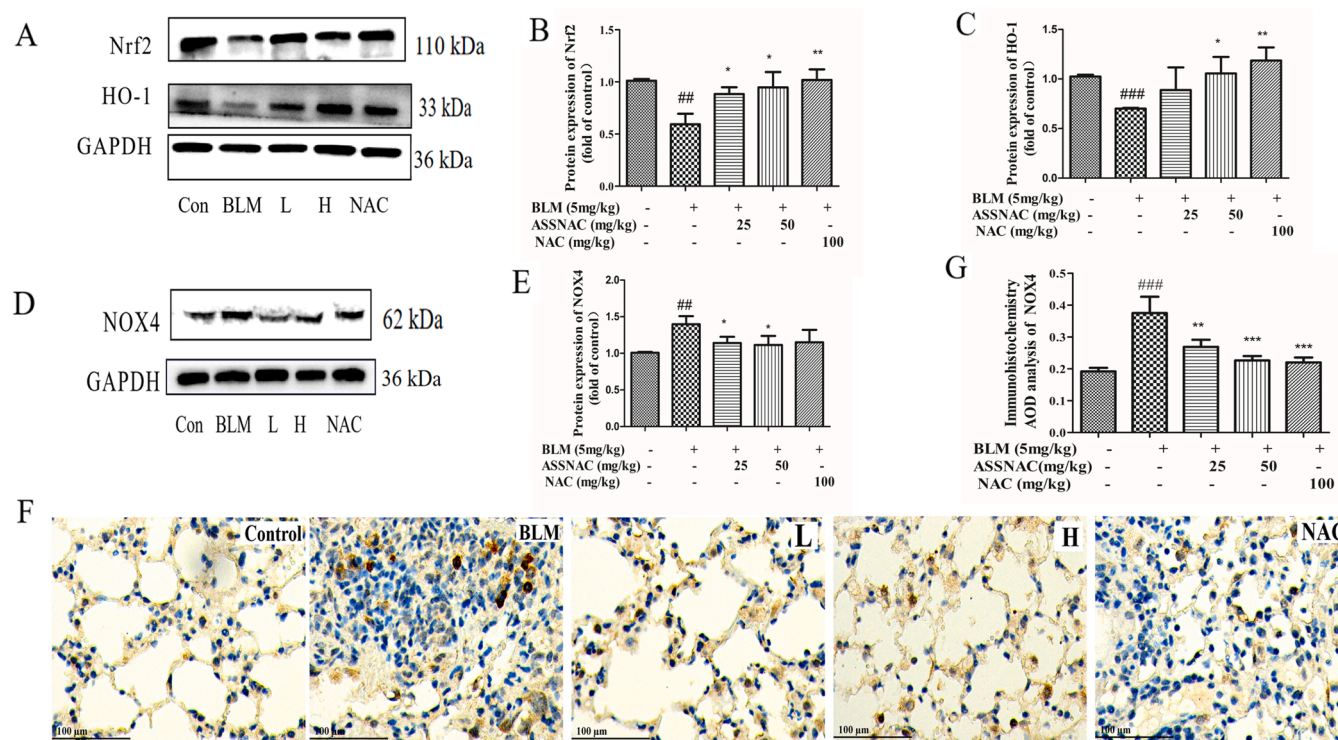
Fig. 7. The effect of ASSNAC against fibrosis through Nrf2 signaling pathway *in vivo*. (A-E) The expressions of Nrf2, HO-1 and NOX4 were checked by Western blot analysis in mice lung with BLM induction and ASSNAC treatment. (F) The protein expression of NOX4 was analysed by immunohistochemical staining. Scale: 100 μm. (G) The immunohistochemistry AOD analysis of NOX4. Data are shown as the mean ± SD (n = 3). #p < 0.05, ##p < 0.01, ###p < 0.001 compared with the control group; *p < 0.05, * *p < 0.01, * **p < 0.001 vs the model group.

significantly reduced in the ASSNAC or NAC treated group compared with the BLM group. In addition, IL-6 and TNF-α levels in BALF were determined (Fig. 8C, D). Compared with the control group, IL-6 and TNF-α remarkably increased in the BLM group, while treatment with ASSNAC or NAC decreased. Consequently, ASSNAC reduces inflammation, which is beneficial to ameliorating PF in mice.

3.8. ASSNAC blocks NF-κB signaling pathway in vivo and in vitro

Since the NF-κB signaling pathway could activate various inflammatory cytokines expressions, it is considered the key inflammatory signaling pathway. To analyse the anti-inflammatory mechanism of ASSNAC, the proteins' expression of NF-κB signaling pathway were tested by Western blot analysis in vivo and in vitro. *In vitro*, the results showed that the expression level of NF-κB p65 was markedly elevated with TGF-β1 stimulated group than control group, while the group treatment with both ASSNAC and NAC significant decrease the levels of NF-κB p65. Compared with TGF-β1 group, the levels of IκB-α was increased significantly after treatment with ASSNAC or NAC (Fig. 6F-H). *In vivo* experiments, compared with the control group, the expressions of p-NF-κB p65 and NF-κB p65 remarkably increase in the BLM group. Conversely, the IκB-α level decreases in the model group. However, it becomes the opposite in the treatment group with ASSNAC or NAC (Fig. 8E-H). Thus, ASSNAC could play an anti-inflammatory role by blocking the NF-κB p65 signaling pathway. This demonstrates that ASSNAC leads to anti-fibrosis by blocking the inflammatory pathways.

3.9. ASSNAC blocks TGF-β1/Smad2/3 signaling pathway in vivo and in vitro

Because the TGF-β1/Smad pathway is activated in the BLM-induced fibrosis [50], it is necessary to understand whether ASSNAC affects the TGF-β1/Smad signaling activation through immunohistochemical and

Western blot analyses. The immunohistochemical results indicate that TGF-β1 and p-Smad2 significantly increased in the model group with BLM treatment but decreased after ASSNAC or NAC treatment in mice lung tissues (Fig. 9A, B). Furthermore, the Western blot analysis examined the expressions of TGF-β1, p-Smad2/3, and Smad2/3 in vivo *and in vitro*. *In vitro,* ASSNAC could inhibit TGF-β1-induced phosphorylation levels of Smad2 and Smad3 (Fig. 6I-K). *In vivo,* the results reveal that ASSNAC could attenuate BLM-induced phosphorylation of Smad2 and Smad3 and the TGF-β1 levels, consistent with immunohistochemical analysis (Fig. 9C-F). Furthermore, the TGF-β1 level in BALF also demonstrates that BLM stimulation leads to TGF-β1 production, but it could be inhibited by ASSNAC or NAC treatment (Fig. 9G). Thus, ASSNAC could block the TGF-β1/Smad2/3 signaling pathway to alleviate PF.

4. Discussion

PF is a chronic and progressive disease leading to rapid and fatal respiratory failure caused by environmental and genetic factors [51]. In the early stage, oxidative stress and continuous inflammation are the main reasons for PF, and fibroblasts transform into myofibroblasts gradually in the later stage [52]. Hence, reducing oxidative stress, inhibiting inflammatory reactions, and fibroblast differentiation are effective strategies for PF. Previous studies have demonstrated that ASSNAC could reduce oxidative stress and inhibit inflammation [37,39]. Also, ASSNAC reduced inflammation was caused by COPD [39,53]. Thus, the therapeutic potential of ASSNAC as an anti-oxidative and anti-inflammatory agent for PF was studied.

TGF-β1 is the main regulator factor of ECM accumulation and EMT in PF [54]. TGF-β1 stimulation can promote the transformation of fibroblasts into myofibroblasts *in vitro,* which influence the expression of α-SMA and extracellular matrix proteins such as collagen I [55]. Therefore, the PF model was established by TGF-β1 stimulated HFL-1 cells to investigate the anti-fibrotic effect of ASSNAC *in vitro*. The
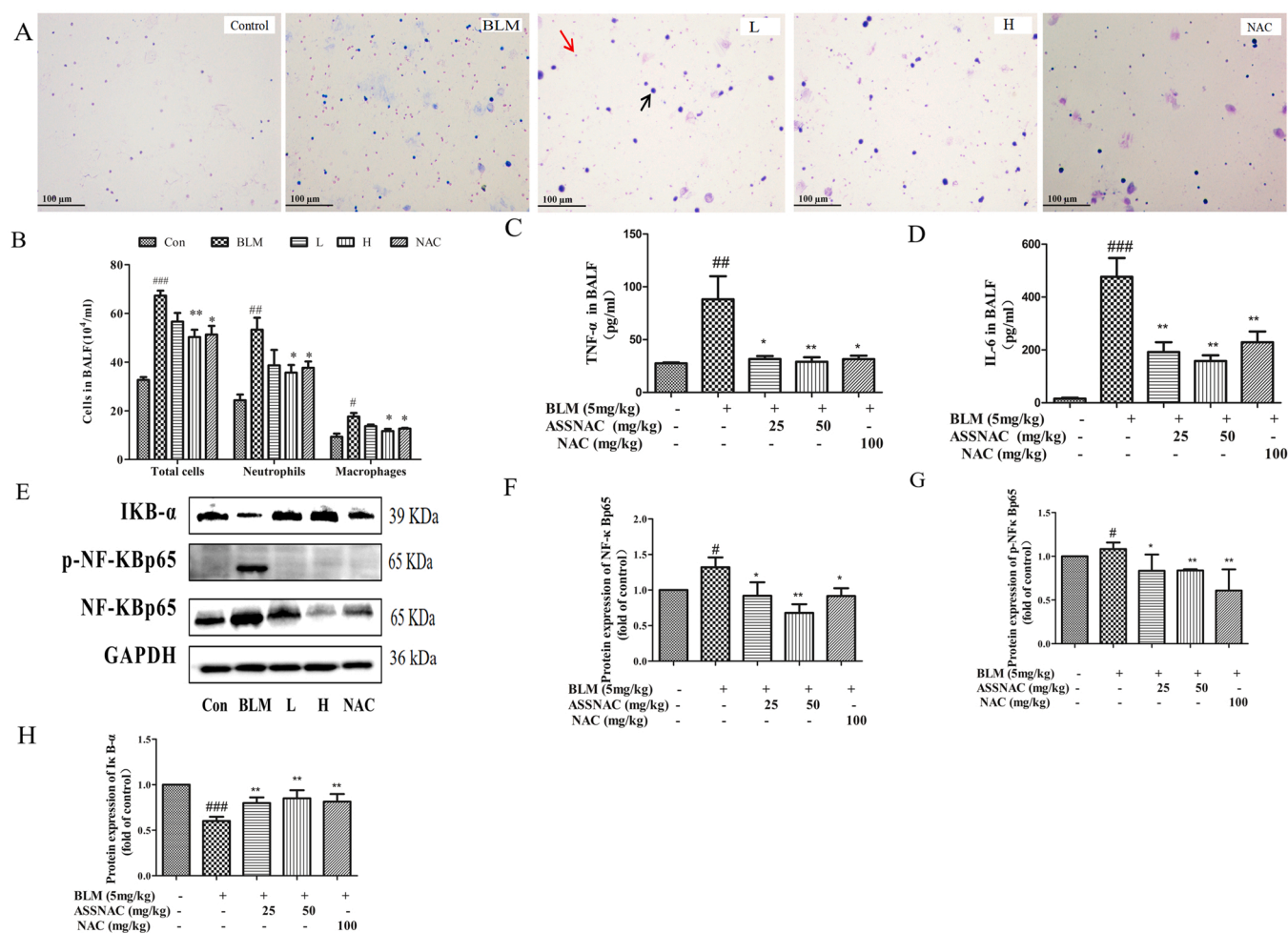
Fig. 8. The effect of ASSNAC alleviated fibrosis through an anti-inflammatory effect. (A, B) The inflammatory cells in BALF were stained by Wright-Giemsa and counted. The red mark is neutrophils and the black mark is macrophages. Scale: 100 μm. (C, D) The IL-6 and TNF-α levels in BALF were tested. (E-H) The protein levels of the NF-κB signaling pathway comprising IkB-α, p-NF-κB p65, and NF-κB p65 were detected in mouse lungs with BLM induction and ASSNAC treatment by Western blot analysis. Data are shown as the mean ± SD (n = 3). #p < 0.05, ##p < 0.01, ###p < 0.001 compared with the control group; *p < 0.05, * *p < 0.01, * **p < 0.001 vs the BLM group.

results demonstrate that ASSNAC inhibits the migration of HFL-1 cells (Fig. 1C, D), the transformation of fibroblasts into myofibroblasts and the expression of α-SMA and collagen I *in vitro* (Fig. 2). Hence, ASSNAC exhibits the anti-fibrotic potential *in vitro*.

Bleomycin, a cytotoxic drug, forms a complex with metal ions and molecular oxygen. These complexes generated ROS in lung tissue and caused PF. This direct oxidative damage with BLM stimulated in lung tissue was followed by an inflammatory response and fibrotic alterations [56]. Hence, BLM is used to cause PF in experiment [57]. The pathological changes in lung tissue and the protein levels of PF are important factors reflecting PF. In the lung tissue with PF, the alveolar structure are destroyed, a large number of inflammatory cells infiltrate and collagen deposition. It has been observed that ASSNAC significantly reduced the infiltration of inflammatory cells, remarkably improved alveolar structure and fibrosis (Fig. 3 A-C). The expression of α-SMA and extracellular matrix proteins including collagen I and III reflect the degree of fibrosis in lung tissue. The results showed that ASSNAC reversed the protein levels of collagen I, collagen III and α-SMA (Fig. 4). Thus, ASSNAC could markedly reduce collagen deposition in BLM-stimulated mouse lungs and alleviates PF.

Various pulmonary diseases and pathological conditions are attributed to oxidative stress [58]. It has been proven that BLM stimulation could advance oxidative stress damage and accelerate ROS production [59]. Chronic inflammatory pulmonary illness and BLM-induced PF are

both accompanied by diminished activity of GSH, a crucial constituent of antioxidant defence systems [60,61]. SOD also is a crucial component of antioxidant defence systems. The reduction of superoxide radical (O_2) was catalyzed into hydrogen peroxide (H_2O_2) by SOD, which reaction helps maintain the redox balance. This study confirms that ASSNAC improves the GSH and SOD levels and follows dose dependence. ASSNAC contains the structure of cysteine, which is an important part of GSH synthesis *in vivo*. It is speculated that ASSNAC provides GSH to the organism, which indirectly affects the SOD level and consequently improves the cells' ability against oxidative stress, as proved in earlier studies [62–64].

PF may be caused by the imbalance between oxidation and anti-oxidation. Thus, activating the anti-oxidative signaling pathway might be an effective solution for PF. ROS are generated by the electron transfer of nicotinamide adenine dinucleotide phosphate (NADPH) oxidase to oxygen, which NADPH requires catalysed through NOXes containing seven subunits [65]. ROS accumulation is mainly attributed to the NOX4 isoform [66]. NOX4 plays a key role in regulating the proliferation and differentiation of fibroblasts and the apoptosis of epithelial cells [67]. The outcome displays that the expression of NOX4 is significantly increased in the model group than in the control group, which reverses with ASSNAC treatment in vivo *and in vitro*. (Fig. 6D-E, Fig. 7D-G). Hence, ASSNAC remarkably affects anti-oxidation and anti-fibrosis by inhibiting the expression of NOX4.
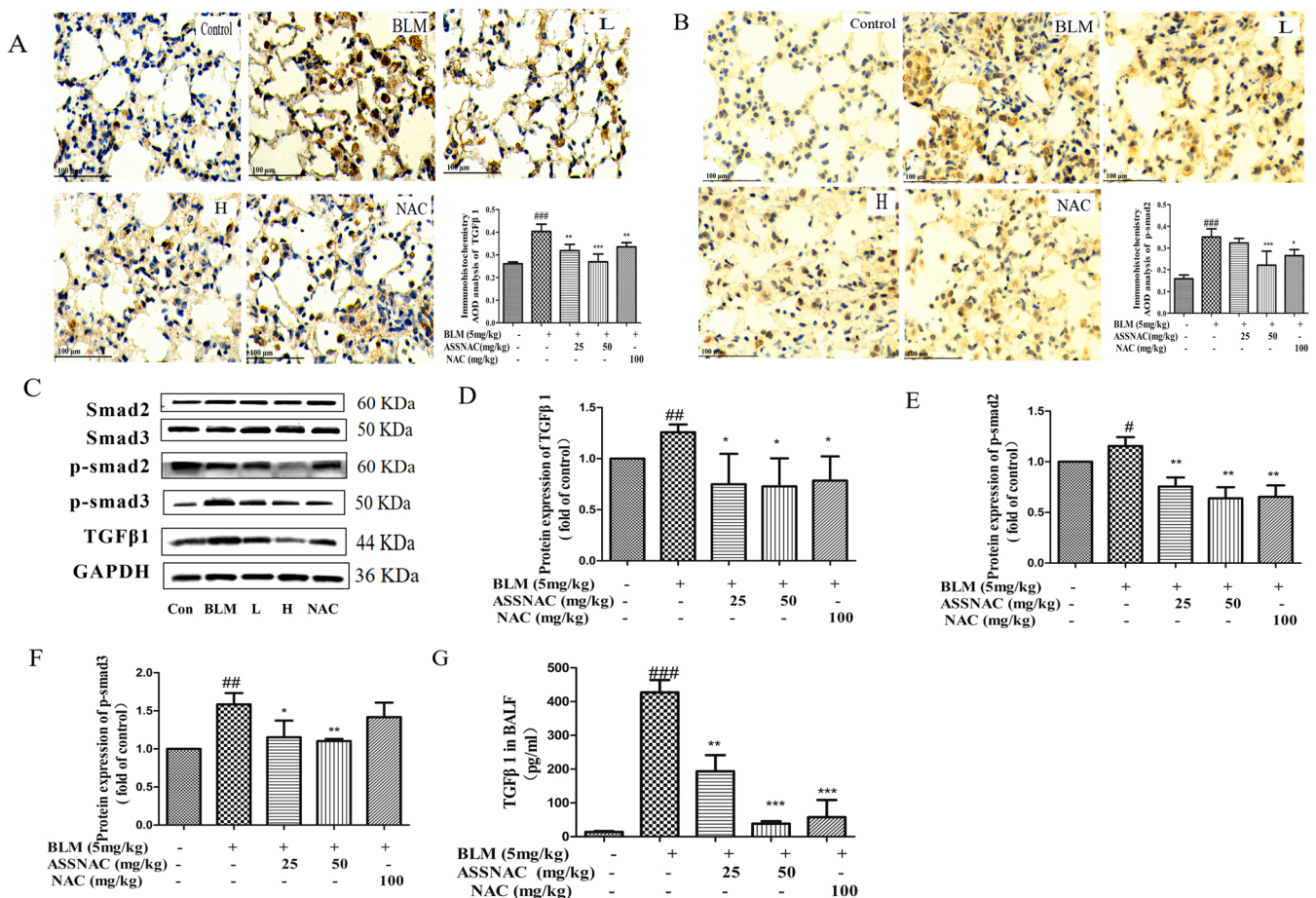
Fig. 9. The effect of ASSNAC alleviated fibrosis through TGF-β1/Smad2/3 signaling pathway. (A-B) The protein expressions of TGF-β1 and p-Smad2 were analysed by immunohistochemical staining. Scale: 100 μm. (C-F) The protein levels of the TGF-β1/Smad2/3 signaling pathway were detected by Western blot analysis in mouse lungs with BLM induction and ASSNAC treatment. (G) The TGF-β1 in BALF content was measured. Data are shown as the mean ± SD (n = 3). #p < 0.05, ##p < 0.01, ###p < 0.001 compared with the control group; *p < 0.05, * *p < 0.01, * **p < 0.001 vs the BLM group.

The activation of the Nrf2 signaling pathway is extremely important for fighting against oxidative stress and exerting protective effects in fibrosis. After the Nrf2 signaling pathway is activated, Nrf2 binds to anti-oxidative response element (ARE) in the cell nucleus, promoting the up-regulation of HO-1 and GCLM [39]. Nrf2 signaling pathway is activated, increasing the anti-oxidant levels such as SOD to keep the intracellular redox balance [68]. ASSNAC significantly increased the Nrf2 and HO-1 levels in vivo *and in vitro* (Fig. 6A-C, Fig. 7A-C). Dose dependence is not remarkable, which may be caused by Western Blot semi-quantitative test error. ASSNAC molecule is a modified cysteine, including NAC and S-allyl mercaptan conjugated by a disulfide bond. Hence, a thiol-exchange reaction could exist between ASSNAC and the free cysteine residue on the oxidative stress sensor of Keap1, causing Nrf2 to release from the Keap1-Nrf2 complex. Thus, ASSNAC probably alleviates PF by activating Nrf2/NOX4 anti-oxidative pathway.

BLM-induced PF causes an inflammatory reaction in the lung tissue and activates the fibrosis axis subsequently. In regulating the expression of inflammatory factors, NF-κB has been considered the most important transcription factor. Generally, NF-κB forms a complex with the inhibitory subunit and remains inactive in the cytoplasm. Nevertheless, once the organism is provoked by inflammatory stimulation, IκB-α is phosphorylated and degrades by ubiquitin-dependent proteasomes. However, NF-κB dissociates from IκB-α and migrates to the nucleus, motivating the cytokines transcription, such as IL-6 and TNF-α [69,70]. Thus, to further investigate the anti-inflammatory activity of ASSNAC, this study examines the contents of inflammatory cells and the levels of pro-inflammatory cytokines containing TNF-α and IL-6 in BALF. The

results show that the contents of inflammatory cells and TNF-α and IL-6 levels significantly reduced after ASSNAC treatment. Also, ASSNAC effectively up-regulated the IκB-α level and down-regulated the NF-κB p65 and p-NF-κB p65 levels in PF mice lungs. Therefore, it could be inferred that ASSNAC plays an anti-inflammatory role by reducing the phosphorylation of IκB-α to block the NF-κB signaling pathway.

In the progression of PF, TGF-β plays a vital role in promoting epithelial cells mesenchymal transition and differentiation of fibroblasts into myofibroblasts [71]. TGF-β1 induces fibroblasts to transform into myofibroblasts, a key event in PF development. The TGF-β1 levels in BALF and lung tissue were increased significantly with BLM induction, and ASSNAC reversed this (Fig. 9C, D, G). Smad2 and Smad3 are two main downstream regulators which promote tissue fibrosis with TGF-β-mediation. In the cytoplasm, Smad proteins are phosphorylated under the stimulation of activated TGF-β, and then the activated Smad2/3 proteins transfer into the nucleus and regulate the transcriptions of target genes [72]. The phosphorylation levels of Smad2 and Smad3 were significantly reduced by ASSNAC treatment (Fig. 6I-K, Fig. 9C, E, F). Hence, it could be concluded that ASSNAC alleviates PF by blocking the TGF-β1/Smad2/3 signaling pathway.

In summary, it is demonstrated that ASSNAC could alleviate PF with BLM-induced mice by fighting against oxidative stress, reducing inflammation and inhibiting fibroblast differentiation. We infer that ASSNAC provides cysteine for GSH synthesis and fights against oxidation imbalance through activating signaling pathway, to reduce inflammation and pulmonary fibrosis subsequently. Based on its potential, it is expected to become a promising new drug for PF treatment.

Besides, adopting an inhalable form to deliver ASSNAC-Na into the lung has unique advantages of improving bioavailability, reducing adverse gastrointestinal effects, and avoiding the first-pass effect on the liver compared with oral administration. Hence, this study on ASSNAC might provide new pathways for PF therapy in the future.

Funding

CRediT authorship contribution statement

Qinxiu Zhang: Investigation, Validation, Writing – original draft. **Wenhui Ye**: Validation. **Ying Liu**: Validation. **Decao Niu**: Validation. **Xin Zhao**: Validation. **Genju Li**: Resources (synthesize ASSNAC and ASSNAC-Na). **Ying Qu**: Writing – review & editing. **Zhongxi Zhao**: Project administration, Supervision, Writing – review & editing.

Conflict of interest statement

The authors declare that they have no known competing financial interests or personal relationships.

Data Availability

The data that has been used is confidential.

Appendix A. Supporting information

Supplementary data associated with this article can be found in the online version at doi:10.1016/j.biopha.2022.114018.

References

[1] G. Raghu, H.R. Collard, J.J. Egan, et al., An official ATS/ERS/JRS/ALAT statement: idiopathic pulmonary fibrosis: evidence-based guidelines for diagnosis and management, Am. J. Respir. Crit. Care Med. 183 (2) (2011) 788–824.

[2] D. Lynch, J. Lynch, T. King, et al., American Thoracic Society. Idiopathic pulmonary fibrosis: diagnosis and treatment. International consensus statement. American Thoracic Society (ATS), and the European Respiratory Society (ERS), Am. J. Respir. Crit. Care Med. 161 (2) (2000) 646–664.

[3] G. Raghu, D. Weycker, J. Edelsberg, et al., Incidence and prevalence of idiopathic pulmonary fibrosis, Am. J. Respir. Crit. Care Med. 174 (7) (2006) 810–816.

[4] P. Lu, J. Li, C. Liu, et al., Salvianolic acid B dry powder inhaler for the treatment of idiopathic pulmonary fibrosis, Asian J. Pharm. Sci. 17 (4) (2022) 475–612.

[5] C.P. Zhao, H. Li, X.H. Liu, et al., Dissecting the underlying pharmaceutical mechanism of Danggui Buxue decoction acting on idiopathic pulmonary fibrosis with network pharmacology, TMR 5 (4) (2020) 14.

[6] Q. Liu, R. Wang, G. Qu, Y. Wang, P. Liu, Y. Zhu, et al., General observation report of systemic anatomy of New Coronavirus Pneumonia deaths, J. Forensic Med. 36 (2020) 19–21.

[7] K.C. Meyer, Pulmonary fibrosis, part I: epidemiology, pathogenesis, and diagnosis, Expert Rev. Respir. Med. 11 (5) (2017) 343–359.

[8] Du, Bois, Roland, et al., Efficacy and safety of nintedanib in idiopathic pulmonary fibrosis, New Engl. J. Med. 370 (2014) 2071.

[9] M. Mehrabani, M. Goudarzi, S. Mehrzadi, A. Siahpoosh, M. Mohammadi, H. Khalili, et al., Crocin: a protective natural antioxidant against pulmonary fibrosis induced by bleomycin, Pharmacol. Rep. 72 (2020) 992–1001.

[10] V. Della Latta, A. Cecchettini, S. Del, R.M.A. Morales, Bleomycin in the setting of lung fibrosis induction: from biological mechanisms to counteractions, Pharm. Res 97 (2015) 122–130.

[11] A. Moeller, K. Ask, D. Warburton, J. Gauldie, M. Kolb, The bleomycin animal model: a useful tool to investigate treatment options for idiopathic pulmonary fibrosis? Int. J. Biochem. Cell Biol. 40 (2008) 362–382.

[12] P. Chitra, G. Saiprasad, R. Manikandan, G. Sudhandiran, Berberine attenuates bleomycin induced pulmonary toxicity and fibrosis via suppressing NF-κB dependant TGF-β activation: a biphasic experimental study, Toxicol. Lett. 219 (2) (2013) 178–193.

[13] K. Bernard, N.J. Logsdon, V. Miguel, G.A. Benavides, J. Zhang, A.B. Carter, et al., NADPH oxidase 4 (nox4) suppresses mitochondrial biogenesis and bioenergetics in lung fibroblasts via a nuclear factor erythroid-derived 2-like 2 (nrf2)-dependent pathway, J. Biol. Chem. 292 (7) (2017) 3029.

[14] M. Mcmahon, K. Itoh, M. Yamamoto, J.D. Hayes, Keap1-dependent proteasomal degradation of transcription factor Nrf2 contributes to the negative regulation of antioxidant response element-driven gene expression, J. Biol. Chem. 278 (24) (2003) 21592–21600.

[15] L. Baird, D. Lleres, S. Swift, A.T. Dinkova-Kostova, Regulatory flexibility in the Nrf2-mediated stress response is conferred by conformational cycling of the Keap1-Nrf2 protein complex, Proc. Natl. Acad. Sci. U. S. A. 110 (2013) 15259–15264.

[16] A.T. Dinkova-Kostova, R.V. Kostov, P. Canning, Keap1, the cysteine-based mammalian intracellular sensor for electrophiles and oxidants, Arch. Biochem. Biophys. 617 (2017) 84–93.

[17] L. Baird, S. Swift, D. Lleres, A.T. Dinkova-Kostova, Monitoring keap1-Nrf2 interactions in single live cells, Biotechnol. Adv. 32 (2014) 1133–1144.

[18] W.B. Zhang, F. Yang, Y. Wang, F.Z. Jiao, H.Y. Zhang, L.W. Wang, Z.J. Gong, et al., Inhibition of HDAC6 attenuates LPS-induced inflammation in macrophages by regulating oxidative stress and suppressing the TLR4-MAPK/NF-κB pathways, Biomed. Pharmacother. 117 (2019), 109166.

[19] B. Li, Z. Cheng, X. Sun, X. Si, E. Gong, Y. Wang, et al., Lonicera caerulea L. polyphenols alleviate oxidative stress-induced intestinal environment imbalance and lipopolysaccharide-induced liver injury in HFD-fed rats by regulating the Nrf2/HO-1/NQO1 and MAPK pathways, Mol. Nutr. Food Res. 64 (2020), 1901315.

[20] L. Hecker, N.J. Logsdon, D. Kurundkar, A. Kurundkar, K. Bernard, T. Hock, et al., Reversal of persistent fibrosis in aging by targeting nox4-nrf2 redox imbalance, Sci. Transl. Med. 6 (231) (2014) 231ra47.

[21] A. Panday, M.E. Inda, P. Bagam, M.K. Sahoo, D. Osorio, S. Batra, Transcription factor NF-κB: an update on intervention strategies, Arch. Immunol. Ther. Exp. 64 (6) (2016) 463–483.

[22] R.M. Mansouri, E. Baugé, B. Staels, P. Gervois, Systemic and distal repercussions of liver-specific peroxisome proliferator-activated receptor-alpha control of the acutephase response, Endocrinology 149 (6) (2008) 3215–3223.

[23] R. Stienstra, S. Mandard, N.S. Tan, W. Wahli, C. Trautwein, T.A. Richardson, et al., The Interleukin-1 receptor antagonist is a direct target gene of PPARalpha in liver, J. Hepatol. 46 (5) (2007) 869–877.

[24] X. Dong, B. Zhao, R.E. Iacob, J. Zhu, A.C. Koksal, C. Lu, J.R. Engen, T.A. Springer, Force interacts with macromolecular structure in activation of TGF-β, Nature 542 (7639) (2017) 55–59.

[25] M. Lodyga, B. Hinz, TGF-beta1 - a truly transforming growth factor in fibrosis and immunity, Semin. Cell Dev. Biol. 101 (2019) 123–139.

[26] J. Hu, Y. Chen, Y. Huang, Y. Su, Human umbilical cord mesenchymal stem cellderived exosomes suppress dermal fibroblasts-myofibroblats transition via inhibiting the TGF-beta1/Smad 2/3 signaling pathway, Exp. Mol. Pathol. 115 (104468) (2020).

[27] G. Chitra, R. Saiprasad, G. Manikandan, Sudhandiran, Berberine attenuates bleomycin induced pulmonary toxicity and fibrosis via suppressing NF-κB dependant TGF-β activation: a biphasic experimental study, Toxicol. Lett. 219 (2) (2013) 178–193.

[28] M. Kolb, F. Bonella, L. Wollin, Therapeutic targets in idiopathic pulmonary fibrosis, Respir. Med. 131 (2017) 49–57.

[29] H. Mojiri-Forushani, A.A. Hemmati, M.A. Dehghani, A.R. Malayeri, H.H. Pour, Effects of herbal extracts and compounds and pharmacological agents on pulmonary fibrosis in animal models: a review, J. Integr. Med. 15 (6) (2017) 433–441.

[30] M. Selman, T.E. King, A. Pardo, Idiopathic pulmonary fibrosis: Prevailing and evolving hypotheses about its pathogenesis and implications for therapy, Ann. Intern. Med. 134 (2) (2001) 136–151.

[31] Y. Cui, H. Xin, Y. Tao, Arenaria kansuensis attenuates pulmonary fibrosis in mice via the activation of Nrf2 pathway and the inhibition of NF-κB/TGF-β1/Smad2/3 pathway, Phytother. Res. 35 (2021) 974–986.

[32] K. Zhang, P. Lu, H. Qin, et al., Traditional Chinese medicine combined with pulmonary drug delivery system and idiopathic pulmonary fibrosis: rationale and therapeutic potential, Biomed. Pharmacother. 133 (111072) (2021). ISSN 0753-3322.

[33] H.H. Mansour, M. Omran, H.F. Hasan, et al., Modulation of bleomycin-induced oxidative stress and pulmonary fibrosis by N-acetylcysteine in rats via AMPK/SIRT1/NF-κβ, Clin. Exp. Pharmacol. Physiol. 47 (2020) 1943–1952.

[34] L. Borgström, B. Kågedal, O. Paulsen, Pharmacokinetics of N-acetylcysteine in man, Eur. J. Clin. Pharmacol. 31 (1986) 217–222.

[35] M. Cazzola, L. Calzetta, C. Page, J. Jardim, A.G. Chuchalin, P. Rogliani, M. G. Matera, Influence of N-acetylcysteine on chronic bronchitis or COPD exacerbations: a meta-analysis, Eur. Respir. Rev. Off. J. Eur. Respir. Soc. 24 (2015) 451–461.

[36] R. He, W. Zheng, T. Ginman, H. Ottosson, S. Norgren, Y. Zhao, M. Hassan, Pharmacokinetic profile of N-acetylcysteine amide and its main metabolite in mice using new analytical method, Eur. J. Pharm. Sci. 143 (2020), 105158.

[37] N. Savion, N. Izigov, M. Morein, et al., S-Allylmercapto-N-acetylcysteine (ASSNAC) protects cultured nerve cells from oxidative stress and attenuates experimental autoimmune encephalomyelitis, Neurosci. Lett. 583 (2014) 108–113.

[38] N. Savion, A. Levine, S. Kotev-Emeth, et al., S-allylmercapto-N-acetylcysteine protects against oxidative stress and extends lifespan in Caenorhabditis elegans, PLOS ONE 96 (13) (2016). S26-S26.

[39] D. Zheng, J. Wang, G. Li, et al., Preliminary therapeutic and mechanistic evaluation of S-allylmercapto-N-acetylcysteine in the treatment of pulmonary emphysema, Int. Immunopharmacol. 98 (2021), 107913.

[40] C.Y. Li, X. Sun, A. Li, M. Mo, Z.X. Zhao, S-Allylmercaptocysteine attenuates Bleomycin-induced pulmonary fibrosis in mice via suppressing TGF-β1/Smad and oxidative stress pathways, Int. Immunopharmacol. 79 (2020), 106110.

[41] N. Izigov, N. Farzam, N. Savion, S-allylmercapto-N-acetylcysteine up-regulates cellular glutathione and protects vascular endothelial cells from oxidative stress, Free Radic. Biol. Med. 50 (9) (2011) 1131–1139.

[42] C. Starkenmann, Y. Niclass, M. Troccaz, Nonvolatile S-alk (en) ylthio-L-cysteine derivatives in fresh onion (Allium cepa L. cultivar), J. Agric. Food Chem. 59 (17) (2011) 9457–9465.

[43] J. He, H. Peng, M. Wang, et al., Isoliquiritigenin inhibits TGF-β1-induced fibrogenesis through activating autophagy via PI3K/AKT/mTOR pathway in MRC-5 cells, ABBS 52 (8) (2020) 11.

[44] X. Li, H. Yu, L. Liang, et al., Myricetin ameliorates bleomycin-induced pulmonary fibrosis in mice by inhibiting TGF-β signaling via targeting HSP90β - ScienceDirect, Biochem. Pharmacol. (2020) 178.

[45] M.R. Corboz, J. Zhang, D. Lasala, et al., Therapeutic administration of inhaled INS1009, a treprostinil prodrug formulation, inhibits bleomycin-induced pulmonary fibrosis in rats, Pulm. Pharmacol. Ther. 49 (2018) 95–103.

[46] B.C. Willis, Z. Borok, TGF-β-induced EMT: mechanisms and implications for fibrotic lung disease, Am. J. Physiol. 293 (3) (2007) 525–534.

[47] R. William, Coward, Gauri, et al., The pathogenesis of idiopathic pulmonary fibrosis, Ther. Adv. Respir. Dis. 4 (6) (2010) 367–388.

[48] J. Morry, W. Ngamcherdtrakul, W. Yantasee, Oxidative stress in cancer and fibrosis: Opportunity for therapeutic intervention with antioxidant compounds, enzymes, and nanoparticles, Redox Biol. 11 (C) (2017) 240–253.

[49] P. Xinyan, D. Chongshan, L. Quanwen, et al., Curcumin attenuates on carbon tetrachloride-induced acute liver injury in mice via modulation of the Nrf2/HO-1 and TGF-β1/Smad3 pathway, Molecules 23 (1) (2018) 215.

[50] V.D. Latta, A. CeCchettini, S.D. Ry, et al., Bleomycin in the setting of lung fibrosis induction: from biological mechanisms to counteractions, Pharmacol. Res. 97 (2015) 122–130.

[51] E.G. Phimister, R.K. Albert, D.A. Schwartz, Revealing the secrets of idiopathic pulmonary fibrosis, New Engl. J. Med. 380 (1) (2019) 94–96.

[52] P.J. Wolters, H.R. Collard, K.D. Jones, Pathogenesis of idiopathic pulmonary fibrosis, Annu. Rev. Pathol. 9 (2014) 157–179.

[53] A.D.B. Jw, A. Gl, et al., S -Allylmercapto -N -acetylcysteine ameliorates elastase-induced chronic obstructive pulmonary disease in mice via regulating autophagy, Biochem. Biophys. Res. Commun. 562 (2021) 83–88.

[54] S.H. Wettlaufer, J.P. Scott, R.C. Mceachin, M. Petersgolden, S.K. Huang, Reversal of the transcriptome by prostaglandin E2 during myofibroblast dedifferentiation, Am. J. Respir. Cell Mol. Biol. 54 (1) (2016) 114.

[55] A. Allawzi, H. Elajaili, E.F. Redente, E. Nozik-Grayck, Oxidative toxicology of bleomycin: role of the extracellular redox environment, Curr. Opin. Toxicol. 13 (2019) 68–73.

[56] C.J. Scotton, R.C. Chambers, Bleomycin revisited: towards a more representative model of IPF? Am. J. Physiol. Lung Cell. Mol. Physiol. 299 (2010) L439–L441.

[57] K.K. Kim, D. Sheppard, H.A. Chapman, TGF-β1 signaling and tissue fibrosis, Cold Spring Harb. Perspect. Biol. (2017), a022293.

[58] Esra, Birben, PhD, et al., Oxidative Stress and Antioxidant Defense. World Allergy Organization Journal. 5(1) (2012) 9–19.

[59] C. Teixeira, F.S. Soares, L. Rocha, et al., Attenuation of bleomycin-induced lung injury and oxidative stress by N-acetylcysteine plus deferoxamine, Pulm. Pharmacol. Ther. 21 (2) (2008) 309–316.

[60] H. Kalantar, E. Sadeghi, F. Abolnezhadian, M. Goudarzi, A.A. Hemmati, Z. Basir, M. Kalantar, Carnosol attenuates bleomycin-induced lung damage via suppressing fibrosis, oxidative stress and inflammation in rats, Life Sci. 287 (2021), 120059.

[61] E. Zinellu, A. Zinellu, Glutathione peroxidase in stable chronic obstructive pulmonary disease: a systematic review and meta-analysis, Antioxidants 10 (11) (2021) 1745.

[62] N. Savion, R. Abu-Kheit, S. Kotev-Emeth, et al., S-allylmercapto-N-acetylcysteine protects caenorhabditis elegans and cultured stromal bone marrow cells from oxidative stress and improves bone microarchitecture of healthy and diabetic mice, Free Radic. Biol. Med. 100 (2016) S109.

[63] N. Savion, N. Izigov, M. Morein, et al., S-allylmercapto-N-acetylcysteine (ASSNAC) up-regulates brain glutathione level and attenuates experimental autoimmune encephalomyelitis, Free Radic. Biol. Med. 51 (supp-S) (2011). S97-S97.

[64] N. Izigov, N. Farzam, N. Savion, S-allylmercapto-N-acetylcysteine up-regulates cellular glutathione and protects vascular endothelial cells from oxidative stress, Free Radic. Biol. Med. 50 (9) (2011) 1131–1139.

[65] E.C. Chan, et al., Regulation of cell proliferation by NADPH oxidase-mediated signaling: potential roles in tissue repair, regenerative medicine and tissue engineering, Pharmacol. Ther. 122 (2) (2009) 97–108.

[66] N. Amara, D. Goven, F. Prost, et al., NOX4/NADPH oxidase expression is increased in pulmonary fibroblasts from patients with idiopathic pulmonary fibrosis and mediates TGFbeta1-induced fibroblast differentiation into myofibroblasts, Thorax 65 (8) (2010) 733–738.

[67] S. Carnesecchi, C. Deffert, Y. Donati, O. Basset, B. Hinz, O. Preynat-Seauve, et al., A key role for nox4 in epithelial cell death during development of lung fibrosis, Antioxid. Redox Signal. 15 (3) (2011) 607–619.

[68] C.C. Abreu, L.F. Cardozo, M, F, D. Mafra, Could physical exercises modulate Nrf2-Keap1 pathway in chronic kidney disease? Med. Hypotheses 84 (1) (2015) 44–46.

[69] A.L. Alessandri, L.P. Sousa, C.D. Lucas, A.G. Rossi, V. Pinho, M.M. Teixeira, Resolution of inflammation: mechanisms and opportunity for drug development, Pharmacol. Ther. 139 (2013) 189–212.

[70] X. Fan, W. Changyuan, J. Yue, et al., Luteolin Protects HUVECs from TNF-alpha-induced Oxidative Stress and Inflammation via its Effects on the NOX4/ROS-NF-κB and MAPK Pathways, J. Atheroscler. Thromb. 21 (8) (2014) 768–783.

[71] X. Song, W. Liu, S. Xie, et al., All-transretinoic acid ameliorates bleomycin-induced lung fibrosis by downregulating the TGF-β1/Smad3 signaling pathway in rats, Lab. Investig. 93 (11) (2013) 1219–1231.

[72] J. Breton, D. Heydet, L.M. Starrs, et al., Molecular changes during TGFβ-mediated lung fibroblast-myofibroblast differentiation: implication for glucocorticoid resistance, Physiol. Rep. 6 (7) (2018), e13669.